Applied Physics Letters ARTICLE scitation.org/journal/apl

Photovoltaic characterizing method of degradation of polymer light-emitting diodes based on ideality factor and density of states

Cite as: Appl. Phys. Lett. **119**, 123301 (2021); doi: 10.1063/5.0057615
Submitted: 22 May 2021 · Accepted: 2 September 2021 ·
Published Online: 21 September 2021

Jaehoon Kim,[a] Taesoo Lee, Jeonghun Kwak, and Changhee Lee[a]

AFFILIATIONS

Department of Electrical and Computer Engineering, Inter-university Semiconductor Research Center, Seoul National University, Seoul 08826, South Korea

[a]Authors to whom correspondence should be addressed: jplane@snu.ac.kr and chlee7@snu.ac.kr

ABSTRACT

Polymer light-emitting diodes (PLEDs) possess several unique advantages over competitive technologies, including solution processability, broad applicability, and low-cost fabrication. However, their commercialization is delayed due to the relatively low operation stability compared to current display techniques. To provide fundamental insight into the degradation mechanism and enhance the stability, we discuss unique analysis methods of PLEDs' degradation using photovoltaic impedance characteristics. In particular, we report the method to determine the energetic disorder or density of states (DOS) of PLEDs using light intensity (P_{light})-dependent open-circuit voltage (V_{OC}) and Cole–Cole plot measurement. Based on the method, it was found that PLED degradation results in a shift of the center of DOS rather than broadening. Furthermore, we extrapolated equivalent ideality factor (n) values from the P_{light}-dependent V_{OC} and dark current density–voltage (J–V) characteristics, which implied trap-assisted recombination throughout the degradation process. Thus, we believe that the results will provide helpful and comprehensive insight into understanding the degradation of PLEDs.

Polymer light-emitting diodes (PLEDs) are one of the candidates for next-generation display due to their solution-processability,[1,2] broad applicability,[3,4] and low-cost fabrication.[2,5,6] Since the PLED was reported in the field, various studies have been conducted to improve the performance. In particular, the synthesis of efficient polymers,[7,8] interfacial engineering,[9] and structural modification[10,11] has contributed to a significant enhancement of the PLEDs' efficiency. However, the commercialization of the PLED has been hindered due to the relatively low operational stability compared to the current display technologies such as thermally evaporated small molecule organic light-emitting diodes (OLEDs).[12,13] The primary reasons for the PLEDs' lower performance than OLEDs or inorganic light-emitting diodes (LEDs) are mainly based on the susceptible degradation of polymers.[14–17] In addition, the impurities and particles in the solutions act as defect sites, limiting the performance of the solution-processed devices.[18] Though many articles reported diverse stability-enhancing methods such as interfacial engineering[19] and stable polymers,[20] systematic analysis on the PLEDs' degradation has been lacking. Specifically, regarding the PLEDs, effective analysis methods have been lacking compared to the solar cells' field, where impedance spectroscopy provides various analysis methods.[21–27]

In this article, we discuss a unique method of analyzing the PLED degradation with photovoltaic properties. Although the PLEDs generally adopt materials with significantly lower charge carrier mobility than organic solar cells' case,[28,29] it is revealed that the photovoltaic measurement methods are applicable to PLEDs, where they provided unique analyzing methods. In particular, comprehensive studies, including the photovoltaic properties and impedance spectroscopy, effectively provided the density of states (DOS) properties of PLEDs. While the characterizing method has been frequently reported in the solar cells' case,[23–27] its application to the PLED has been missing, which would make interesting and valuable tools in PLED studies. As it is reported in the solar cell articles,[23] the capacitance components of the emissive layer (EML) (an active layer in the case of solar cells) were extrapolated from the Cole–Cole plots under diverse open-circuit conditions with various light intensity (P_{light}) circumstances. The capacitance as a function of the bias V_{OC} generally shows an apparent Gaussian-shaped DOS, providing essential insight into the organic solar cells' (OSCs) energy level characteristics. Similarly, it is found that the method applies to the PLED as well, where the variation in DOS, a significant shift of the center of DOS, was measured upon degradation. In addition to the DOS-related analyses, we also offer a

systematic study on the ideality factor (n) using both the P_{light}-dependent open-circuit voltage (V_{OC}) and the dark current density– voltage (J–V). Although the ideality factor (n) has been widely adopted in the PLEDs' area,[30] a systematic study that comprises the comprehensive analyses of both P_{light}-dependent V_{OC} and dark J–V has been rarely reported. However, by a complete examination, the equivalent values from both methods and the importance of the cross verification are confirmed.

The structure of PLEDs was ITO/ZnO NP/PEIE/PDY-132/MoO_X/Al [Fig. 1(a)], where the respective abbreviations are indium tin oxide (ITO), ZnO nanoparticle (ZnO NP), and polyethyleneimine ethoxylated (PEIE). The detailed experimental methods are summarized in the supplementary material. The energy band diagram is calculated based on ultraviolet photoelectron spectroscopy (UPS) (Figs. S1 and S2) and a Tauc plot (Fig. S3). The electroluminescent characteristics of PLEDs were measured in terms of current density–voltage–luminance (J–V–L) characteristics, electroluminescence (EL) spectrum, current efficiency (CE), luminance stability, and driving voltage stability (Fig. 1). Assuming the turn-on voltage (V_{on}) as the voltage of which luminance is 1 cd m^{-2}, V_{on} showed a value of 2.8 V. The maximum CE was 10.3 cd A^{-1} at J of 24.3 mA cm^{-2}. The vibronic EL peaks were distinguished at the wavelength of 556 and 587 nm, which corresponds to the S_{0-0} and S_{0-1} transitions, respectively.[31] Upon degradation, the respective peaks at 556 and 587 nm showed no change in the shape of normalized EL spectra (Fig. S4). According to former articles, aging polymer causes aggregation of the polymer chains, resulting shoulder peaks shifting toward longer wavelengths,[32,33] while the PDY is reported to have stubborn EL spectra compared to other polymers with ignorable change in shape against aging.[34,35] Thus, the identical ratio of peaks of 556–587 nm upon degradation is in good agreement with the former articles. The luminance stability T_{50}, an indication of the time when the luminance drops by

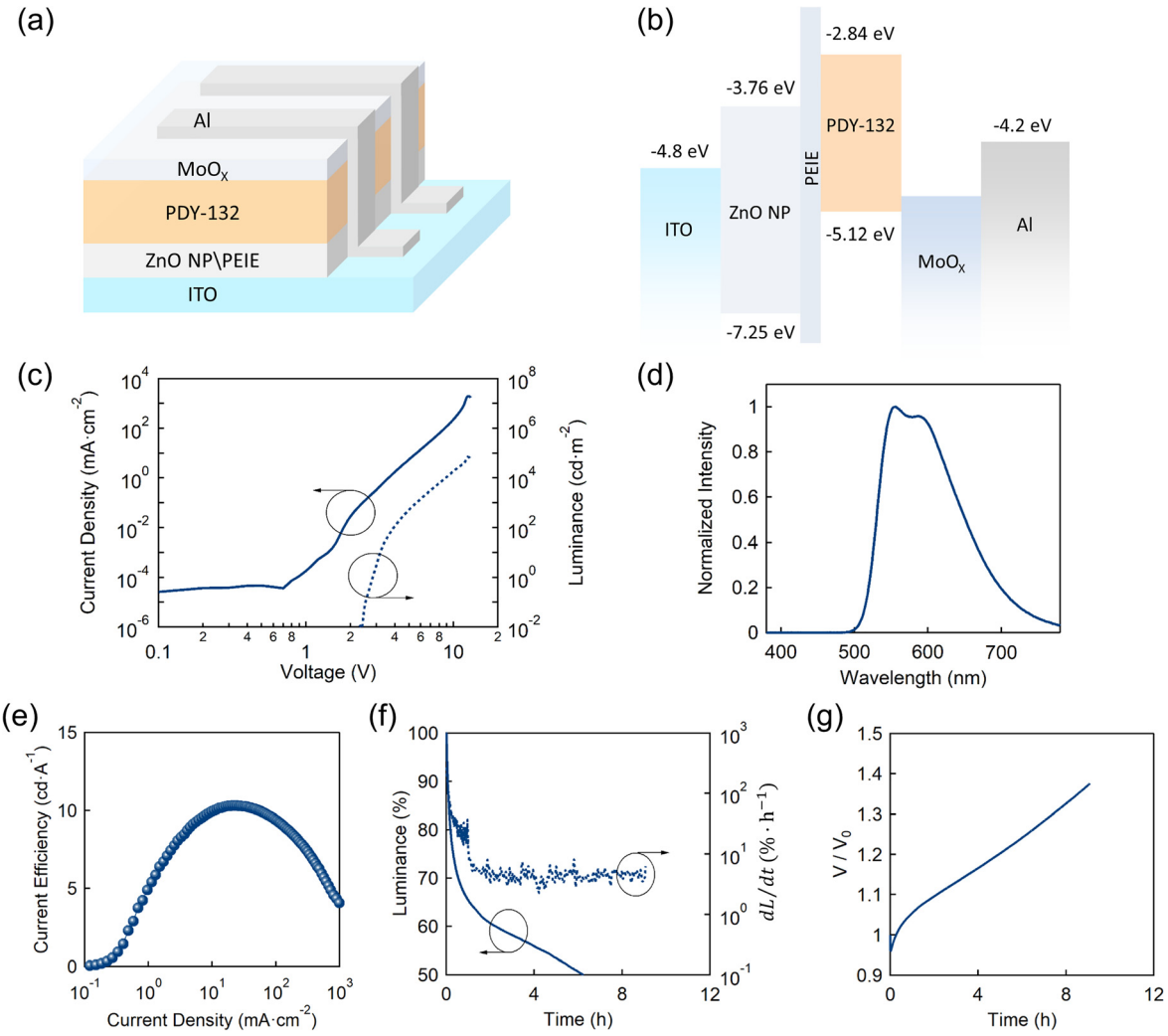

FIG. 1. (a) Device architecture and (b) energy band diagram of PLEDs. (c) J–V–L characteristics, (d) normalized electroluminescence (EL) spectrum, (e) current efficiency (CE), variation of (f) luminance and differential luminance and (g) normalized driving voltage under constant current with an initial luminance of 1000 cd m^{-2} without any encapsulation.

50%, showed a value of 6.2 h. The initial luminance was 1000 cd m^{-2}, corresponding to the current density of 9.95 mA cm^{-2}. The stability was measured in an ambient condition without encapsulation for acceleration and magnification of the degradation effect, resulting in rapid deterioration. For comparison of device performance with former articles, devices with encapsulation were also fabricated and evaluated (Fig. S5). While the PLEDs showed no difference in initial performance, showing a CE of 10.6 cd A^{-1}, the T_{50} of PLEDs with encapsulation is expected to exceed 500 h through the fitting. Furthermore, the encapsulated device showed significantly enhanced stability of the driving voltage, a 1.15-fold increase by 365 h, whereas the unencapsulated one offered a 1.25-fold increase by 9 h (Fig. S6). The devices showed significantly variant stability depending on the encapsulation (Fig. S6), agreeing with the former articles reporting the detrimental effect of air exposure on organic devices.[36] Therefore, it can be concluded that the device efficiency and operational stability are comparable with that of former articles.[35] In line with the luminance stability, the driving voltage increased by 25% after 6.2 h. Based on the device degradation results, we systematically investigate the photovoltaic characteristics of PLEDs as follows.

In Fig. 2, the *J*–*V* characteristics of PLEDs were measured upon degradation as a function of varying P_{light} from 100 to 0.32 mW cm^{-2}. From the *J*–*V* characteristics, the parameters of the short-circuit current (J_{SC}), open-circuit voltage (V_{OC}), fill factor (FF), and power conversion efficiency (PCE) were calculated. In line with the previous articles in photovoltaics, the *J*–*V* curve showed variation upon P_{light}.[37] Under 100 mW cm^{-2} illumination, the pristine and aged PLEDs' photovoltaic characteristics were J_{SC} = 3.14 μA cm^{-2}, V_{OC} = 1.67 V, FF = 0.31, and PCE = 1.65×10^{-3}% and J_{SC} = 2.25 μA cm^{-2}, V_{OC} = 1.52 V, FF = 0.33, and PCE = 1.14×10^{-3}%, respectively (Table I). As the photovoltaics degraded in terms of respective photovoltaic parameters (J_{SC}, V_{OC}, FF, and PCE), the PLED showed relevant variation upon degradation where J_{SC} decreased from 3.14 to 2.25 μA cm^{-2} and V_{OC} decreased from 1.67 to 1.52 V, which resulted in a PCE drop by 31%. In order to analyze the fundamentals, the J_{SC} was measured as a function P_{light}, which offered insight into the recombination mechanism within the device [Eq. (1)][37]

$$J_{SC} \propto P_{light}^{\alpha}, \tag{1}$$

$$V_{OC} = \frac{E_g}{q} - \frac{nkT}{q} \ln\left[\frac{(1-P_D)\gamma N_C^2}{P_D G}\right]. \tag{2}$$

According to numerous former articles in photovoltaics,[37] it is generally known that the J_{SC} shows a linear dependence to the P_{light} for an ideal case. In other words, all generated electron and hole pairs are effectively transported, showing nothing but only monomolecular recombination with α close to 1 [Eq. (1)]. However, disadvantageous phenomena, including space-charge effect, charge imbalance, and bimolecular recombination, hinder effective charge transport, decreasing the α down to 0.75 to the minimum.[37] The PLED before and after degradation showed α of 0.92 and 1.05, respectively [Fig. 2(c)]. Therefore, we can speculate that the charges are well extracted without any space charge effect, charge imbalance, and bimolecular recombination.

To analyze in more depth, we plotted the P_{light}-dependent V_{OC}, which provided information regarding trap-assisted recombination within the device [Fig. 2(d)]. In brief, the V_{OC} shows a linear dependence to the natural logarithm of P_{light} [Eq. (2)]. In detail, E_g is the energy bandgap, q is the elementary charge, n is the ideality factor, k is the Boltzmann constant, T is the temperature in kelvin, P_D is the dissociation probability, γ is the Langevin recombination constant, N_C is the effective DOS, and G is the generation rate. In particular, the ideality factor (n) reveals the charge recombination environment within the device. In the general photovoltaics case, the ideality factor (n) is close to 1, while it increases up to 2 to the maximum.[37] Contrary to the short-circuit condition where monomolecular recombination is dominant [Fig. 2(c)], the bimolecular recombination becomes the dominant recombination mechanism in the open-circuit condition [Fig. 2(d)]. In an open-circuit condition, the ideality factor (n) equals 1 when only the bimolecular recombination is involved. In the general case, the ideality factor (n) increases to 2 as additional trap-assisted recombination starts to evolve. However, the PLEDs showed an ideality factor over 2 in Fig. 2(d). In particular, the ideality factor (n) was 4.36 for the pristine device, which decreased to 2.53 after degradation. Although the general range of the ideality factor is between 1 and 2, it can exceed the range significantly because of several reasons such as recombination, leakage current, trap-assisted tunneling, and inhomogeneous junctions.[38–41] In line with the argument, several articles report organic diodes, including OLEDs with the ideality factor (n) significantly higher than 2 (Table SI).[39,42–46] Nguyen *et al.* reported that the OLEDs based on both evaporation and solution processes show significantly a high ideality factor (n) over 24,[39] which can originate from trap-assisted tunneling, carrier leakage, or inhomogeneous junctions among layers. Similarly, Na *et al.* reported that the ideality factor (n) of OLEDs increased from 6.3 to 9.98 upon thermal stress for temperature over the glass transition temperature (T_g), which accompanied an abrupt increase in the characteristic trap energy.[46] Based on the former studies, we can conclude that a significant amount of recombination or leakage current is involved in the PLED in the pristine state. However, after degradation, the ideality factor (n) decreased to 2.53, implying a reduced amount of trap-assisted recombination within the device.[37,47–49] Nonetheless, the value still exceeds 2 after degradation, revealing that the trap-assisted recombination continuously occurred during the entire aging process, where only the relative amount of degradation has been reduced. It also agrees well with the differential luminance degradation trend in Fig. 1(f). Since the luminance dropped sharply at first and started to slow down after a while, we can see that the time-differential luminance was higher at first and

TABLE I. Photovoltaic performance parameters and resistive components of the PLED before and after aging.

	J_{SC} (μA cm^{-2})	V_{OC} (V)	FF	PCE ($\times 10^{-3}$%)	R_S (Ω cm^2)	R_{SH} (Ω cm^2)
Pristine	3.14	1.67	0.31	1.65	1.68×10^5	6.33×10^5
Aged	2.25	1.52	0.33	1.14	1.38×10^5	7.91×10^5

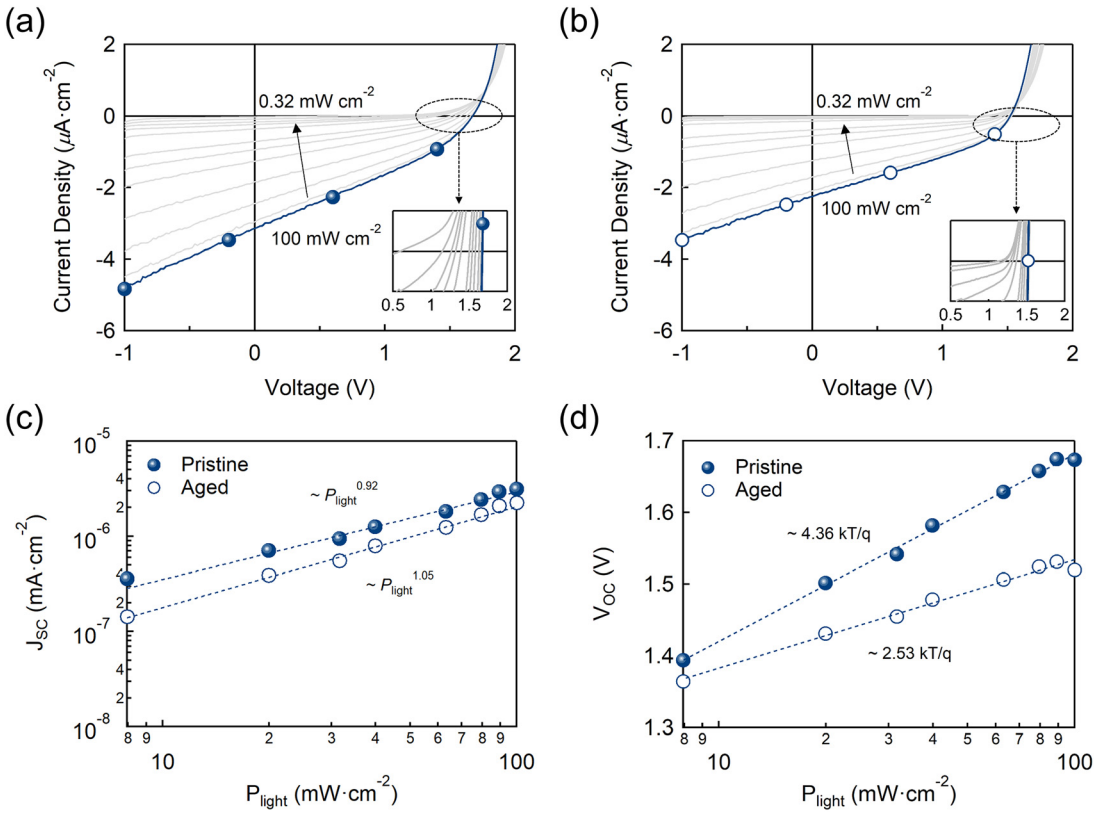

FIG. 2. Photovoltaic *J–V* characteristics of the (a) pristine and (b) aged PLEDs as a function of P_{light} varying from 100 to 0.32 mW cm^{-2}. Variation of P_{light}-dependent (c) J_{SC} and (d) V_{OC} of PLEDs upon degradation.

started to saturate after a while [Fig. 1(f)], which well agrees with the trend of the ideality factor (n) [Fig. 2(d)]. Thus, we can conclude that the amount of the ideality factor over two positively correlates with the time-differential decrease in luminance upon degradation. In the next paragraph, we checked the ideality factor by extrapolating the dark state *J–V* characteristics. Then, we analyzed the *J–V* characteristics variation upon degradation, which provided clues for the significantly high ideality factor in the pristine state

$$n = \left(\frac{kT}{q}\frac{\partial \ln(J)}{\partial V}\right)^{-1}. \quad (3)$$

Previously, various researchers have reported that the *J–V* curve of a diode in the dark state also offers ideality factor (n) [Eq. (3)]. In line with the P_{light}-dependent V_{OC}, dark *J–V* provides a comparable value of the ideality factor (n). The values extracted from both methods must have equivalent value to guarantee the preciseness of the experiment. In Fig. 3(a), the dark *J–V* characteristics of pristine and aged PLEDs are plotted. In particular, we can find out that the pristine PLED showed a higher leakage current, which is believed to be the reason for the higher ideality factor.[38,47,50,51] The leakage current of the pristine PLED showed a significantly high value ranging from 10^{-5} to 10^{-4} mA cm^{-2} before the V_{on}, while the aged PLED showed a significant decrease in the leakage current ranging from 10^{-7} to 10^{-6} mA cm^{-2} before V_{on}. For the decrease in the leakage current after aging is speculated to relate to several former articles, which states a decrease in the leakage current after electrical stress.[52,53] In accordance to the papers, it is argued that electrical stress upon LED devices can induce annealing, which eliminates the deep hole traps at the electron injection layer (EIL)/cathode interface.[52] Furthermore, the higher leakage current of pristine PLEDs than the aged one agrees well with the higher slope of P_{light}-dependent V_{OC} and more severe drop of luminance for the pristine state PLED. Based on Eq. (3), the *J–V* curve-extrapolated ideality factors for pristine and aged devices were 4.07 and 2.63, respectively [Fig. 3(b)]. Considering that the P_{light}-dependent V_{OC}-extrapolated ideality factors (n) were 4.36 and 2.53, the values showed considerable consistency, implying the accuracy of the calculation. Thus, we can confirm that although the ideality factor (n) decreased upon degradation, the overall values were over 2, implying a continuous trap-assisted recombination environment. As discussed, the significant ideality factor (n) of the pristine state is attributed to the large leakage current, and the fundamental reason for the reduced ideality factor during operation is speculated to originate from the removal of disadvantageous mid-gap states by electrical annealing.[52] While the previous results discussed the characterization methods for trap-assisted recombination within the PLEDs, the later paragraphs demonstrate a unique characterization method of PLEDs' degradation based on impedance spectroscopy and DOS.

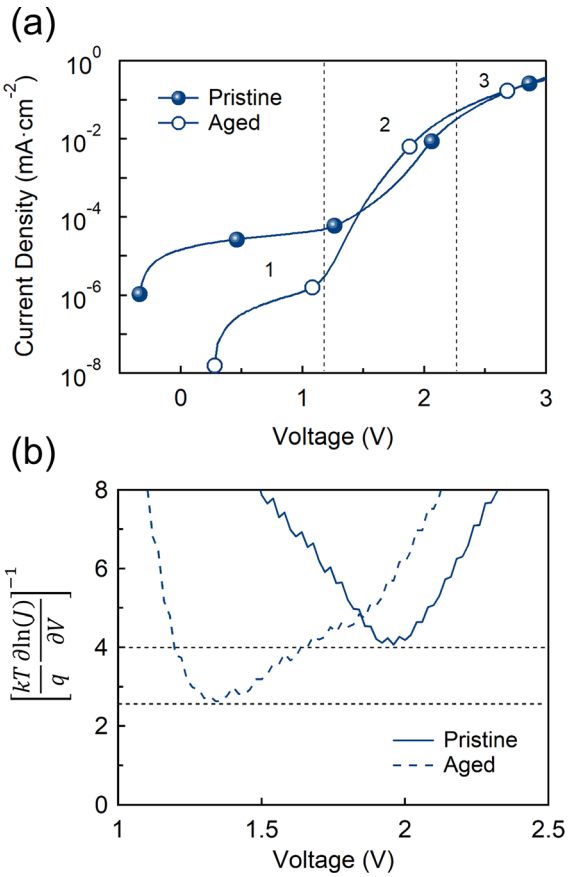

FIG. 3. Variation of (a) dark *J*–*V* characteristics and (b) extrapolated ideality factor of PLEDs upon degradation.

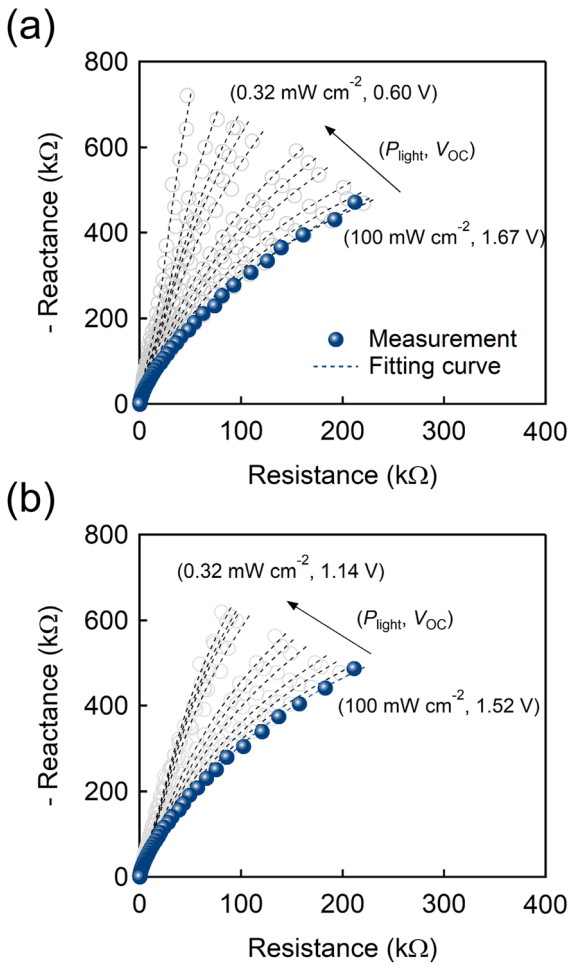

FIG. 4. Cole–Cole plots of (a) pristine and (b) aged PLEDs under respective open-circuit conditions of (P_{light}, V_{OC}).

In Fig. 4, the Cole–Cole plots of the PLEDs were measured with various open-circuit conditions. In the case of OSCs, various researchers have reported that the Cole–Cole plot provides an effective tool for characterizing the DOS using impedance spectroscopy.[28,29] Briefly explaining, considering that the DOS at a given voltage difference within the active layer is proportional to the capacitance, the capacitance values under several open-circuit conditions offer a clear and vivid shape of the DOS. For various conditions of open-circuit conditions, the external light illumination and the bias voltage were varied following the values of P_{light}-dependent V_{OC} values [Fig. 2(d)]. In Fig. 4, the Cole–Cole plots before and after degradation were measured under the light illumination of P_{light} and the bias voltage of V_{OC}. Assuming that the equivalent circuit of the PLEDs consists of serial components of series resistance (R_S) and three parallel *RC* components, the respective resistance and capacitance values are extrapolated and listed in Tables SII and SIII. Among three *RC* components, the resistance of the third *RC* component, denoted as R_3, showed significantly increasing variation upon decreasing P_{light}, implying that the third *RC* component is related to the light-sensitive active layer. Therefore, we can conclude that the capacitance of the third *RC* component, denoted as C_3, represents the capacitance value of the active layer, EML for the PLED, and is proportional to the DOS. Based on the assumption, we plotted the C_3 values as a function of the bias voltage of V_{OC}, which showed an apparent Gaussian shaped-DOS

$$g(E) = \frac{N}{\sqrt{2\pi}\sigma} e^{\left(\frac{(E-E_0)^2}{2\sigma^2}\right)}. \quad (4)$$

In general, the lowest unoccupied molecular orbital (LUMO) exhibits a broad Gaussian-shaped-DOS,[27,54] which leads to a decrease in V_{OC} in solar cells.[55] In Eq. (4), g(*E*) is the DOS upon the electric field, *N* is the charge carrier density, σ is the degree of DOS broadening, and *E* and E_0 are the electric field and center of DOS, respectively. The PLED before and after degradation showed some apparent change in DOS behavior (Fig. 5). In brief, the DOS is calculated based on the linear correlation with the capacitance.[23] While the degree of DOS broadening (σ) barely varied, changing from 711 to 644 mV, the center of DOS (E_0) showed significant variation from 2.16 to 1.77 V. Since the pristine E_0 of 2.16 V is close to the E_g of PDY-132 of 2.28 V [Fig. 1(b)], we can conclude that the DOS measurement of PLEDs showed high accuracy based on the fact that E_0 is highly related to the E_g of the active layer.[23] However, a severe shift of E_0 was observed after

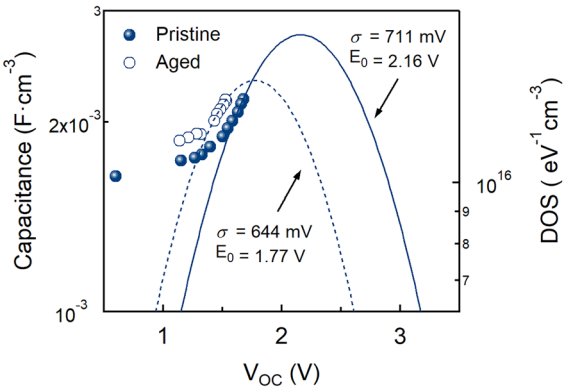

FIG. 5. Variation of capacitance and density of states (DOS) of PLEDs upon degradation.

degradation, changing from 2.16 to 1.77 V, contrary to the unchanged E_g from the EL spectrum after aging (Fig. S4). The inconsistency between E_0 and E_g after aging is speculated to originate from the fact that the characteristics of DOS, including E_0, are affected by comprehensive factors, including not only the E_g of the active layer itself but also the adjacent layer's mid-gap trap states during degradation.[55] Therefore, we can conclude that a considerable decrease in E_0 was observed by the DOS measurement, which provided an effective clue of mid-gap states generation within the PLED.

In conclusion, we discussed the degradation of PLEDs based on unique methods of the ideality factor and DOS, which are based on photovoltaic characterization. The ideality factor (n) of the PLED was obtained through P_{light}-dependent V_{OC} and dark J–V characteristics, and both methods offered consistent values, which imply the accuracy of the extrapolation. Moreover, the ideality factor decreased after degradation, but both pristine and aged ideality factors were above 2, indicating continuous involvement of trap-assisted recombination. Furthermore, impedance spectroscopy was utilized to extrapolate the DOS characteristics of PLEDs. Contrary to the general case of OSCs, it is found that the DOS showed no broadening, whereas the center of the DOS, denoted as E_0, showing a significant shift from 2.16 to 1.77 eV. Regardless of our device results, we believe that our method of analyzing the PLEDs' photovoltaic characteristics will give a helpful insight into studying the degradation of LEDs.

See the supplementary material for the detailed methods of device fabrication and characterization; former articles in OLEDs with high ideality factor (n); extrapolated RC components and DOS from the Cole–Cole plots; UPS and Tauc plot measurement results of ZnO and PDY-132; EL spectra decay upon degradation depending on the encapsulation; device current efficiency and operational stability depending on the encapsulation; and driving voltage stability of PLEDs depending on the encapsulation.

This work was supported by the National Research Foundation of Korea (No. NRF-2016R1A2B3009301) and LG Chem, Ltd.

DATA AVAILABILITY

The data that support the findings of this study are available from the corresponding authors upon reasonable request.

REFERENCES

[1]S.-R. Tseng, S.-C. Lin, H.-F. Meng, H.-H. Liao, C.-H. Yeh, H.-C. Lai, S.-F. Horng, and C.-S. Hsu, Appl. Phys. Lett. **88**, 163501 (2006).
[2]S. Shin, M. Yang, L. J. Guo, and H. Youn, Small **9**, 4036 (2013).
[3]J. Liang, L. Li, K. Tong, Z. Ren, W. Hu, X. Niu, Y. Chen, and Q. Pei, ACS Nano **8**, 1590 (2014).
[4]P. A. Haigh, F. Bausi, Z. Ghassemlooy, I. Papakonstantinou, H. L. Minh, C. Fléchon, and F. Cacialli, Opt. Express **22**, 2830 (2014).
[5]J. Park, H. Yoon, G. Kim, B. Lee, S. Lee, S. Jeong, T. Kim, J. Seo, S. Chung, and Y. Hong, Adv. Funct. Mater. **29**, 1902412 (2019).
[6]H. Zheng, Y. Zheng, N. Liu, N. Ai, Q. Wang, S. Wu, J. Zhou, D. Hu, S. Yu, S. Han, W. Xu, C. Luo, Y. Meng, Z. Jiang, Y. Chen, D. Li, F. Huang, J. Wang, J. Peng, and Y. Cao, Nat. Commun. **4**, 1971 (2013).
[7]X. Zhang, Q. Hu, J. Lin, Z. Lei, X. Guo, L. Xie, W. Lai, and W. Huang, Appl. Phys. Lett. **103**, 153301 (2013).
[8]Y. Wu, X. Li, H. Zhao, J. Li, Y. Miao, H. Wang, F. Zhu, and B. Xu, Org. Electron. **76**, 105487 (2020).
[9]B. R. Lee, E. D. Jung, J. S. Park, Y. S. Nam, S. H. Min, B.-S. Kim, K.-M. Lee, J.-R. Jeong, R. H. Friend, J.-S. Kim, S. O. Kim, and M. H. Song, Nat. Commun. **5**, 4840 (2014).
[10]Q. Zhuang, D. Zou, G. You, K. Li, H. Zhen, and Q. Ling, Nanotechnology **31**, 085201 (2019).
[11]Y. Ma, F. Peng, T. Guo, C. Jiang, Z. Zhong, L. Ying, J. Wang, W. Yang, J. Peng, and Y. Cao, Org. Electron. **54**, 133 (2018).
[12]C.-Y. Chan, M. Tanaka, Y.-T. Lee, Y.-W. Wong, H. Nakanotani, T. Hatakeyama, and C. Adachi, Nat. Photonics **15**, 203 (2021).
[13]L. Cao, K. Klimes, Y. Ji, T. Fleetham, and J. Li, Nat. Photonics **15**, 230 (2021).
[14]F. So and D. Kondakov, Adv. Mater. **22**, 3762 (2010).
[15]B. H. Cumpston, I. D. Parker, and K. F. Jensen, J. Appl. Phys. **81**, 3716 (1997).
[16]V. N. Bliznyuk, S. A. Carter, J. C. Scott, G. Klärner, R. D. Miller, and D. C. Miller, Macromolecules **32**, 361 (1999).
[17]C. Giebeler, S. A. Whitelegg, D. G. Lidzey, P. A. Lane, and D. D. C. Bradley, Appl. Phys. Lett. **75**, 2144 (1999).
[18]A. Jolt Oostra, P. W. M. Blom, and J. J. Michels, Org. Electron. **15**, 1166 (2014).
[19]M. M. Alam and S. A. Jenekhe, Chem. Mater. **14**, 4775 (2002).
[20]G. Jin, L. Xia, Z. Liu, H. Lin, J. Ling, H. Wu, L. Hou, and Y. Mo, J. Mater. Chem. C **4**, 905 (2016).
[21]O. Almora, D. Miravet, G. J. Matt, G. Garcia-Belmonte, and C. J. Brabec, Appl. Phys. Lett. **116**, 013901 (2020).
[22]S. K. Gupta, L. S. Pali, and A. Garg, Sol. Energy **178**, 133 (2019).
[23]G. Garcia-Belmonte, P. P. Boix, J. Bisquert, M. Sessolo, and H. J. Bolink, Sol. Energy Mater. Sol. Cells **94**, 366 (2010).
[24]G. Garcia-Belmonte, P. P. Boix, J. Bisquert, M. Lenes, H. J. Bolink, A. La Rosa, S. Filippone, and N. Martín, J. Phys. Chem. Lett. **1**, 2566 (2010).
[25]Y. Shao, Y. Yuan, and J. Huang, Nat. Energy **1**, 15001 (2016).
[26]F. Fabregat-Santiago, G. Garcia-Belmonte, I. Mora-Seró, and J. Bisquert, Phys. Chem. Chem. Phys. **13**, 9083 (2011).
[27]G. Garcia-Belmonte, Sol. Energy Mater. Sol. Cells **94**, 2166 (2010).
[28]P. W. M. Blom, M. C. J. M. Vissenberg, J. N. Huiberts, H. C. F. Martens, and H. F. M. Schoo, Appl. Phys. Lett. **77**, 2057 (2000).
[29]M. M. Mandoc, L. J. A. Koster, and P. W. M. Blom, Appl. Phys. Lett. **90**, 133504 (2007).
[30]H. T. Nicolai, A. Hof, and P. W. M. Blom, Adv. Funct. Mater. **22**, 2040 (2012).
[31]B. Park, I.-G. Bae, S. Y. Na, Y. Aggarwal, and Y. H. Huh, Opt. Express **27**, A693 (2019).
[32]G. Burwell, N. Burridge, O. J. Sandberg, E. Bond, W. Li, P. Meredith, and A. Armin, Adv. Electron. Mater. **6**, 2000732 (2020).
[33]J. Liu, T.-F. Guo, and Y. Yang, J. Appl. Phys. **91**, 1595 (2002).
[34]S. Burns, J. MacLeod, T. Trang Do, P. Sonar, and S. D. Yambem, Sci. Rep. **7**, 40805 (2017).
[35]S. Stolz, Y. Zhang, U. Lemmer, G. Hernandez-Sosa, and H. Aziz, ACS Appl. Mater. Interfaces **9**, 2776 (2017).
[36]M. Schaer, F. Nüesch, D. Berner, W. Leo, and L. Zuppiroli, Adv. Funct. Mater. **11**, 116 (2001).

[37]A. K. K. Kyaw, D. H. Wang, V. Gupta, W. L. Leong, L. Ke, G. C. Bazan, and A. J. Heeger, ACS Nano **7**, 4569 (2013).
[38]H. T. Nguyen, S. Y. Ryu, A. T. Duong, and S. Lee, RSC Adv. **9**, 38464 (2019).
[39]H. T. Nguyen, A. T. Duong, and S. Lee, Opt. Mater. **111**, 110708 (2021).
[40]Ö. Güllü, Ş. Aydoğan, and A. Türüt, Microelectron. Eng. **85**, 1647 (2008).
[41]Ş. Aydoğan, Ü. İncekara, A. R. Deniz, and A. Türüt, Microelectron. Eng. **87**, 2525 (2010).
[42]S. Ouro Djobo, J. C. Bernède, K. Napo, and Y. Guellil, Mater. Chem. Phys. **77**, 476 (2003).
[43]J. Laubender, L. Chkoda, M. Sokolowski, and E. Umbach, Synth. Met. **111–112**, 373 (2000).
[44]I.-M. Ling and L.-H. Chen, Curr. Appl. Phys. **10**, 346 (2010).
[45]I. Na, S. E. Lee, M.-K. Joo, I.-H. Park, J.-I. Song, H. Joo, Y. K. Kim, and G.-T. Kim, Curr. Appl. Phys. **20**, 78 (2020).
[46]I. Na, K. J. Kim, G.-T. Kim, Y. Seo, Y. Kim, Y. K. Kim, and M.-K. Joo, Appl. Phys. Lett. **117**, 063303 (2020).
[47]G.-J. A. H. Wetzelaer and P. W. M. Blom, NPG Asia Mater. **6**, e110 (2014).
[48]C. H. Kim, O. Yaghmazadeh, Y. Bonnassieux, and G. Horowitz, J. Appl. Phys. **110**, 093722 (2011).
[49]M. Kuik, H. T. Nicolai, M. Lenes, G.-J. A. H. Wetzelaer, M. Lu, and P. W. M. Blom, Appl. Phys. Lett. **98**, 093301 (2011).
[50]D. Zhu, J. Xu, A. N. Noemaun, J. K. Kim, E. F. Schubert, M. H. Crawford, and D. D. Koleske, Appl. Phys. Lett. **94**, 081113 (2009).
[51]G. A. H. Wetzelaer, L. J. A. Koster, and P. W. M. Blom, Phys. Rev. Lett. **107**, 066605 (2011).
[52]R. K. Sharma, M. Katiyar, I. V. K. Rao, K. N. Narayanan Unni, and Deepak, Phys. Chem. Chem. Phys. **18**, 2747 (2016).
[53]F. Pedroli, A. Marrani, M.-Q. Le, O. Sanseau, P.-J. Cottinet, and J.-F. Capsal, RSC Adv. **9**, 12823 (2019).
[54]T. Heumueller, T. M. Burke, W. R. Mateker, I. T. Sachs-Quintana, K. Vandewal, C. J. Brabec, and M. D. McGehee, Adv. Energy Mater. **5**, 1500111 (2015).
[55]J. Kim, H. Jung, J. Song, K. Kim, and C. Lee, ACS Appl. Mater. Interfaces **9**, 24052 (2017).